Prof. Wei Yi
Associate Editor
IEEE Transactions on Signal Processing

March 10, 2025

**Response to Decision on Manuscript T-SP-32387-2024**

Dear Editor and Reviewers,

We sincerely appreciate your feedback provided during the review process of T-SP-32387-2024. Your comments and suggestions have been invaluable in helping us improve the quality of the manuscript. Below we prepare a point-to-point response and highlight the corresponding in-text changes, where labels have been matched to the latest version for your convenience. The title has been changed to *MIMO Channel Shaping and Rate Maximization Using Beyond Diagonal RIS* to better reflect the content of the manuscript. We hope that the revisions and clarifications make the manuscript meet the standards of TSP publications.

Yours sincerely,

Yang Zhao, Hongyu Li, Bruno Clerckx, and Massimo Franceschetti

## Editorial Decision

The reviewers raised a number of concerns regarding the paper's contribution, novelty, and mathematical correctness, which led to the recommendation for rejection. The main issues identified include:

(a) The contribution of the paper is unclear. Specifically, the proposed framework in (25) is not sufficiently general as it does not consider Beyond Diagonal (BD)-Reconfigurable Intelligent Surface (RIS) dependent constraints (e.g., Quality of Service (QoS), sensing quality). A more general case has already been investigated and solved in the authors' previous work [36]. Some content in Section III-B are well established methods in the literature [49].

(b) The optimization problems (39) and (36) lacks of novelty. The reviewer pointed that they can be possibly solved by existing methods through appropriate adjustment [i, 28]. Also, it is also pointed out that Corollaries 3.1 – 3.2 are the standard results from matrix textbook.

(c) The correctness and usefulness of the mathematical derivations. For example, the derivation in the proof of Appendix H is incorrect. Convergence proof in Appendix J is questionable. The usefulness of these bounds on singular values of the effective channel $\mathbf{H}$ is unclear.

(d) The literature review can be enhanced to cover a boarder range of papers that related to the problem addressed.

(e) The simulation study can be enhanced. For example, comparisons with the Diagonal (D)-RIS and a globally passive BD-RIS were suggested by the reviewer.

**Response** We appreciate the editor's summary of the comments. We have carefully considered each point raised and have made significant revisions to address these concerns. Please refer to **1.1** for (a), **1.5** and **1.6** for (b), **1.3** and **1.4** and **1.6** for (c), **1.5** for (d), and **3.3** for (e) in the following responses.

## Reviewer 1

This manuscript investigates the impact of BD-RIS to the distribution of singular values of Multiple-Input Multiple-Output (MIMO) channel of a point-to-point communication system. Especially, the authors derive bounds of singular values of BD-RIS channel and propose algorithms to design BD-RIS configuration.

**1.1** *The contribution of Sec. III-B is unclear for the following two reasons.*

*(a) The manuscript claims to propose a universal optimization framework for BD-RIS as in (25). However, the framework in (25) is indeed not sufficiently general. It does not consider BD-RIS dependent constraints (e.g., QoS, sensing quality) besides the orthogonal conditions (25b). The reviewer notice that a more general framework, which considers BD-RIS constraints in addition to (25b), has already been investigated and solved in the authors' previous work [36].*

*(b) Besides, both the non-geodesic Riemannian Conjugate Gradient (RCG) and geodesic RCG algorithms, e.g., (27) – (33), are well established methods in the literature, e.g., [49]. Therefore, the novelty of Sec. III-B unclear.*

**Response** We appreciate the reviewer's insightful comments. The geodesic RCG algorithm for unitary-constrained problems has indeed been proposed in the optimization literature. Our contribution is an extension to block-unitary cases with parallel or unified updates that accelerate the design of group-connected BD-RIS. The claim of "universal optimization framework" and the non-geodesic RCG method have been removed to avoid confusion, and we have completely reworked the optimization part to reflect the particular contributions (channel shaping). The content is too long to fit here and we kindly ask the reviewer to refer to Section III-B of the revised manuscript for details.

**1.2** *In Sec. III-B, the manuscript proposes to maximize weighted sum of singular values of the effective channel* $\mathbf{H}$*. The optimization objective is rather vague. Is the weighted sum of singular values related to any meaningful performance metric (e.g., capacity, power gain, and so on)?*

**Response** This is an important question. The weighted sum of singular values plays a crucial role in channel shaping since it helps to reveal the achievable singular value region. We believe itself could serve as a metric for measuring the MIMO channel shaping capability of different RIS models. We have added a detailed explanation in the revised manuscript which we copy in the two boxes below.

To validate Algorithm 1 and quantify the shaping capability of BD-RIS, we characterize the achievable singular value region of BD-RIS-aided MIMO channel by considering the Pareto optimization problem

$$\begin{aligned} \max_{\boldsymbol{\Theta}} \quad & \sum_{n=1}^{N} \rho_n \sigma_n(\mathbf{H}) \\ \text{s.t.} \quad & \boldsymbol{\Theta}_g^{\mathsf{H}} \boldsymbol{\Theta}_g = \mathbf{I}, \quad \forall g, \end{aligned}$$

where $\rho_n \geq 0$ is the weight associated with the $n$-th channel singular value. Varying those weights help to characterize the Pareto frontier that encloses the achievable singular value region. While the objective (34a) itself seems obscure, a larger quantity translates to a stronger singular value redistribution capability and thus better wireless performance (e.g., channel capacity for communication [5], detection probability for sensing [54], and harvested power for power transfer [24]). Problem (34) also generalizes the Degrees of Freedom (DoF) problem in Proposition 1 and the individual singular value shaping problem in Corollary 3.3 and Proposition 2. It can be solved optimally by Algorithm 1 with $[\mathbf{D}]_{n,n} = \rho_n$ in (26).

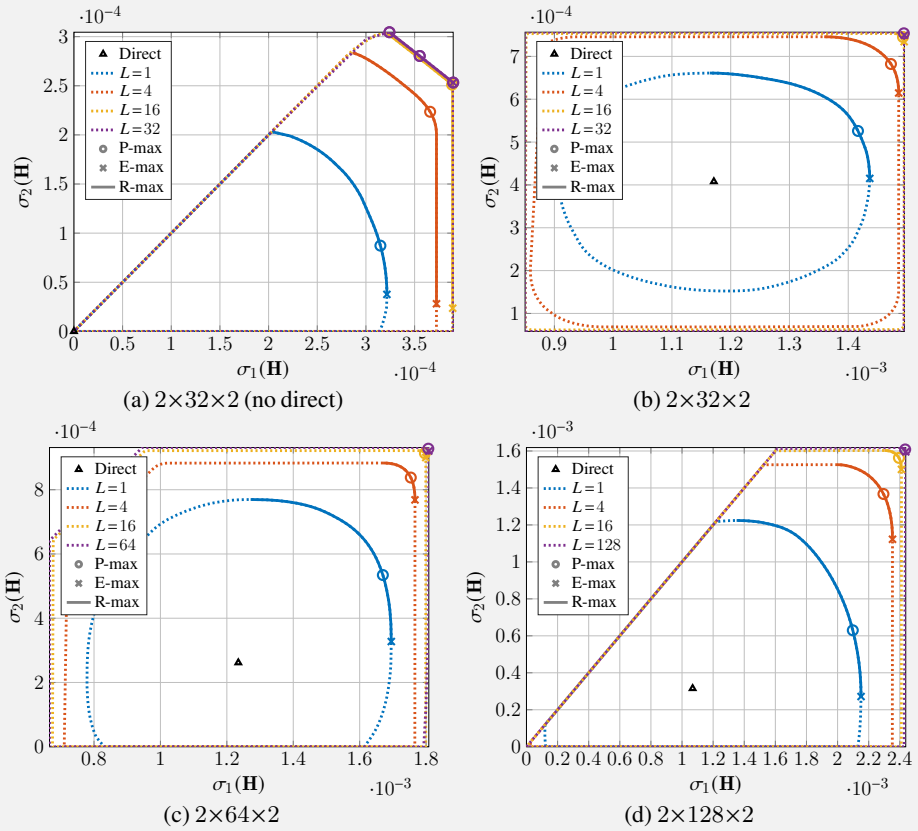


(a) 2×32×2 (no direct) (b) 2×32×2

(c) 2×64×2 (d) 2×128×2

Figure 2: Achievable singular value regions of an $N_{\mathrm{T}} = N_{\mathrm{R}} = 2$ channel shaped by BD-RIS. The singular value pair of the direct channel are marked as baseline. On the Pareto frontiers, 'P-max', 'E-max', and 'R-max' refer to the channel power gain-optimal point, wireless power transfer-optimal point, and rate-optimal arc, respectively.

Fig. 2 illustrates the achievable regions of singular values of an $N_{\mathrm{T}} = N_{\mathrm{R}} = 2$ point-to-point MIMO shaped by RIS, where the channel power gain-optimal point, wireless power transfer-optimal point,[a] and rate-optimal arc are highlighted on the Pareto frontiers. The results are obtained by solving the channel shaping problem (34) merely without any application-specific optimization. As the Signal-to-Noise Ratio (SNR) increases, the rate-optimal point proceeds on the arc from the east (favoring $\sigma_1(\mathbf{H})$) to the north (favoring $\sigma_2(\mathbf{H})$). When the direct channel is negligible, the achievable regions in Fig. 2(a) are shaped like pizza slices. This is because $\sigma_1(\mathbf{H}) \geq \sigma_2(\mathbf{H})$ and there exists a trade-off between the alignment of two modes. The smallest singular value can be enhanced up to $2\times10^{-4}$ by D-RIS and $3\times10^{-4}$ by fully-connected BD-RIS, corresponding to a 50 % gain. We also see that for fully-connected BD-RIS, the power gain-optimal and rate-optimal points coincide with each other, as have been proved in (20a) and (23). This observation still holds in Figs. 2(b) – 2(d) where the direct channel is significant, yet a formal proof is unavailable due to the non-trivial solution structures. The shape of the singular value region depends heavily on the relative strength of the indirect channels, which is $\Lambda_{\mathrm{F}}\Lambda_{\mathrm{B}}/\Lambda_{\mathrm{D}} = -35\mathrm{dB}$ here. Fig. 2(b) shows that a 32-element RIS is insufficient to compensate this imbalance and results in a limited singular value region that is symmetric around the direct point. As the group size $L$ increases, the shape of the region evolves from elliptical to square. This transformation not only improves the dynamic range of $\sigma_1(\mathbf{H})$ and $\sigma_2(\mathbf{H})$ by 22 % and 38 %, but also provides a better trade-off in manipulating both singular values. It verifies that the design flexibility of BD-RIS allows better alignment of multiple modes simultaneously. As a consequence, the optimally shaped channels for power gain, communication, and power transfer coincide, which implies that a fully-connected BD-RIS may be designed in closed-form for multi-functional optimality. The singular value region also enlarges as the number of scattering elements $N_{\mathrm{S}}$ increases. In particular, Fig. 2(d)

shows that the equivalent channel can be completely nulled (corresponding to the origin) by a 128-element BD-RIS but not by a diagonal one, which may be leveraged for interference cancellation and covert communication. Those results demonstrate the superior channel shaping capability of BD-RIS and emphasizes the importance of adding reconfigurable inter-connections between elements.

[a] For MIMO wireless power transfer with Radio Frequency (RF) combining, the maximum harvested power depends solely on the dominant channel singular value [24].

**1.3** *Derivation in the proof of Appendix H is incorrect. Specifically,* $(\partial \mathbf{u}^{\mathsf{T}}) \cdot \mathbf{u}$ *is not equal to* $\partial(\mathbf{u}^T \mathbf{u})$. *Similar error occurs to* $\mathbf{v}$. *Please note that the derivative of singular value of a matrix with respect to the matrix itself does not exist. In fact, sub-differential should be used instead, e.g., [ii].*

**Response** We appreciate the reviewer for pointing out the error. We have corrected the derivation in the proof of Appendix H and have used the sub-differential to handle the non-differentiability of the singular value function.

Consider a special class of channel shaping problem

$$\begin{aligned} \max_{\boldsymbol{\Theta}} \quad & f\big(\mathrm{sv}(\mathbf{H})\big) \\ \text{s.t.} \quad & \boldsymbol{\Theta}_g^{\mathsf{H}} \boldsymbol{\Theta}_g = \mathbf{I}, \quad \forall g, \end{aligned}$$

where $f : \mathbb{R}^N \to \mathbb{R}$ is a symmetric gauge function (i.e., a norm invariant under sign change and argument permutation) [6]. Examples of such $f$ include the Ky Fan $k$ norm, Schatten $p$ norm, $n$-th singular value, and channel power gain. Problem (25) is non-convex due to the unitary constraints (25b) and non-smooth due to the possibility of repeated singular values or singular values crossing each other.

**Proposition 4.** *The sub-differential of (25a) with respect to BD-RIS block* $g$ *is*

$$\partial_{\boldsymbol{\Theta}_g^*} f\big(\mathrm{sv}(\mathbf{H})\big) = \mathrm{conv}\big\{\mathbf{H}_{\mathrm{B},g}^{\mathsf{H}} \mathbf{U} \mathbf{D} \mathbf{V}^{\mathsf{H}} \mathbf{H}_{\mathrm{F},g}^{\mathsf{H}}\big\},$$

*where* $\mathbf{D} \in \mathbb{C}^{N_{\mathrm{R}} \times N_{\mathrm{T}}}$ *is a rectangular diagonal matrix with* $[\mathbf{D}]_{n,n} \in \partial_{\sigma_n(\mathbf{H})} f\big(\mathrm{sv}(\mathbf{H})\big)$, $\forall n \in [N]$, *and* $\mathbf{U}$, $\mathbf{V}$ *are any left and right singular matrices of* $\mathbf{H}$.

**1.4** *The rank equation in the proof of Prop. 1 (Appendix A) seems confusing. The rank of product of two matrices is:* $\mathrm{rank}(\mathbf{AB}) = \mathrm{rank}(\mathbf{B}) - \dim(\ker(\mathbf{A}) \cap \mathrm{ran}(\mathbf{B}))$. *How could one obtain the rank equation in Appendix A? Please clarify.*

**Response** Using the rank equation pointed out by the reviewer, we realized that the achievability proof was invalid and the proposition itself was wrong. We really appreciate the reviewer for pointing out this mistake. A new proof in Appendix A shows that BD-RIS may achieve a larger or smaller number of MIMO DoF than D-RIS. The change in the main text is as follows.

**Proposition 1** (DoF)**.** *BD-RIS may achieve a larger or smaller MIMO DoF than D-RIS.*

*Proof.* Please refer to Appendix A in the supplement. □

While increasing the DoF improves the asymptotic rate performance for point-to-point transmission, the potential to reduce the DoF can be exploited to orthogonalize channels and align interference in multi-user scenarios.

**Example 1** (DoF of $4 \times 4 \times 4$ shaping)**.** Consider a $4 \times 4 \times 4$ shaping with $\mathbf{H}_{\mathrm{D}} = \mathbf{0}$, $\mathbf{H}_{\mathrm{B}} = \begin{bmatrix} 1 & 1 & 0 & 0 \\ 0 & 0 & 0 & 0 \\ 0 & 0 & 1 & 0 \\ 0 & 0 & 0 & 0 \end{bmatrix}$,

and $\mathbf{H}_{\mathrm{F}} = \mathrm{diag}(1,1,0,0)$. Evidently, any D-RIS $\mathbf{\Theta}_{\mathrm{D}} = \mathrm{diag}(e^{\jmath\theta_1}, e^{\jmath\theta_2}, e^{\jmath\theta_3}, e^{\jmath\theta_4})$ results in

$$\mathbf{H} = \begin{bmatrix} e^{\jmath\theta_1} & e^{\jmath\theta_2} & 0 & 0 \\ 0 & 0 & 0 & 0 \\ 0 & 0 & 0 & 0 \\ 0 & 0 & 0 & 0 \end{bmatrix}$$

with 1 DoF. On the other hand, a fully-connected BD-RIS can perfectly align or misalign the kernels of $\mathbf{H}_{\mathrm{B}}$ and $\mathbf{H}_{\mathrm{F}}$ using the closed-form solutions (ii) or (iii) in Appendix A. That is, $\mathbf{\Theta}^{\mathrm{MIMO}}_{\text{DoF-max}} = \begin{bmatrix} 0 & \frac{1}{\sqrt{2}} & 0 & -\frac{1}{\sqrt{2}} \\ 0 & \frac{1}{\sqrt{2}} & 0 & \frac{1}{\sqrt{2}} \\ -1 & 0 & 0 & 0 \\ 0 & 0 & 1 & 0 \end{bmatrix}$ and $\mathbf{\Theta}^{\mathrm{MIMO}}_{\text{DoF-min}} = \begin{bmatrix} -\frac{1}{\sqrt{2}} & 0 & \frac{1}{\sqrt{2}} & 0 \\ \frac{1}{\sqrt{2}} & 0 & \frac{1}{\sqrt{2}} & 0 \\ 0 & 0 & 0 & 1 \\ 0 & -1 & 0 & 0 \end{bmatrix}$, which correspond to

$$\mathbf{H} = \begin{bmatrix} 0 & \sqrt{2} & 0 & 0 \\ 0 & 0 & 0 & 0 \\ -1 & 0 & 0 & 0 \\ 0 & 0 & 0 & 0 \end{bmatrix}, \quad \mathbf{H} = \mathbf{0},$$

and a DoF of 2 and 0, respectively.

Proposition 1 and Example 3 suggest that we can expect more parallel streams or less interference when shaping the channel with BD-RIS. The latter is particularly helpful in multi-user scenarios where the problem of interest is interference alignment or physical layer security. We now take a step further to examine the limits of redistributing channel singular values under specific channel conditions.

**1.5** *In Sec. III-A, the manuscript provides a number of bounds on singular values of the effective channel* $\mathbf{H}$. *However, the usefulness of these bounds is unclear. What can these bounds be used for? Note the results in Corollaries 3.1 – 3.2 are quite standard results from matrix textbook. The (upper) bound in Corollary 3.4, which is achieved by aligning its left and right singular-value vectors to that of the forward and backward channels, respectively, is reminiscent of the results in seminal papers on relay beamforming design, e.g., [iii, iv].*

**Response** We would like to argue that, while Corollaries 3.1 – 3.2 are standard mathematical results, it is Proposition 3 that allows one to recast the channel shaping question as a well-studied linear algebra problem and enable those. We have added a paragraph to reflect this point.

Proposition 3 says that if the direct channel is negligible and the BD-RIS is fully-connected, the only singular value bounds on the equivalent channel are those on the product of unitary-transformed backward and forward channels. It is *not necessarily* an asymptotic result and does *not* depend on any relationship between $N_{\mathrm{R}}$, $N_{\mathrm{S}}$, and $N_{\mathrm{T}}$. Its importance lies in that our initial channel shaping question can be recast as a linear algebra question: *How the singular values of matrix product are bounded by the singular values of its individual factors?* The question is partially answered in Corollaries 3.1 – 3.3 over the definition $\bar{N} = \max(N_{\mathrm{T}}, N_{\mathrm{S}}, N_{\mathrm{R}})$ and $\sigma_n(\mathbf{H}) = \sigma_n(\mathbf{H}_{\mathrm{F}}) = \sigma_n(\mathbf{H}_{\mathrm{B}}) = 0$, $\forall n \in [\bar{N}] \setminus [N]$. This is equivalent to padding zero blocks at the end of $\mathbf{H}, \mathbf{H}_{\mathrm{B}}, \mathbf{H}_{\mathrm{F}}$ to make square matrices of dimension $\bar{N}$. The results are by no means complete and interested readers are referred to [1, Chapter 16, 24] and [42, Chapter 3] for more information.

In the revised manuscript, we have emphasized above and have also added

- Upper and lower bounds on individual singular value in Corollary 3.3;
- Lower bound on channel power gain in Corollary 3.4;
- Upper bound on channel capacity at general SNR in Corollary 3.5 and at extreme SNR in 3.6.

The corresponding RIS scattering matrices have also been derived in closed form. We believe those bounds and RIS expressions not only serve as benchmarks but also motivate low-complexity designs (e.g., Section IV-B) in various wireless applications. For example, the bounds on the $n$-th singular value can be used to

simplify precoding design in MIMO systems with limited number $n$ of RF chains. The comparison to relay beamforming design is insightful and we have added a paragraph to highlight the connection.

**Corollary 3.3** (Individual singular value)**.** *If the direct channel is negligible, then the n-th channel singular value can be manipulated up to*

$$\max_{i+j=n+N_{\mathrm{S}}} \sigma_i(\mathbf{H}_{\mathrm{B}})\sigma_j(\mathbf{H}_{\mathrm{F}}) \le \sigma_n(\mathbf{H}) \le \min_{i+j=n+1} \sigma_i(\mathbf{H}_{\mathrm{B}})\sigma_j(\mathbf{H}_{\mathrm{F}}),$$

*where* $(i,j) \in [N_{\mathrm{S}}]^2$*. The upper and lower bounds are attained respectively at*

$$\begin{aligned}\boldsymbol{\Theta}_{\text{sv-}n\text{-max}}^{\text{MIMO-ND}} &= \mathbf{V}_{\mathrm{B}}\mathbf{P}\mathbf{U}_{\mathrm{F}}^{\mathsf{H}},\\ \boldsymbol{\Theta}_{\text{sv-}n\text{-min}}^{\text{MIMO-ND}} &= \mathbf{V}_{\mathrm{B}}\mathbf{Q}\mathbf{U}_{\mathrm{F}}^{\mathsf{H}},\end{aligned}$$

*where* $\mathbf{V}_{\mathrm{B}}, \mathbf{U}_{\mathrm{F}} \in \mathbb{U}^{N_{\mathrm{S}}\times N_{\mathrm{S}}}$ *are any right and left singular matrices of* $\mathbf{H}_{\mathrm{B}}$ *and* $\mathbf{H}_{\mathrm{F}}$*, respectively, and* $\mathbf{P}$ *and* $\mathbf{Q}$ *are arbitrary permutation matrices of dimension* $N_{\mathrm{S}}$ *satisfying:*

- *The* $(i,j)$*-th entry is* $1$*, where*

$$(i,j) = \begin{cases} \operatorname*{argmin}_{i+j=n+1} \sigma_i(\mathbf{H}_{\mathrm{B}})\sigma_j(\mathbf{H}_{\mathrm{F}}), & \text{for } \mathbf{P},\\ \operatorname*{argmax}_{i+j=n+N_{\mathrm{S}}} \sigma_i(\mathbf{H}_{\mathrm{B}})\sigma_j(\mathbf{H}_{\mathrm{F}}), & \text{for } \mathbf{Q}. \end{cases}$$

  *and ties may be broken arbitrarily;*

- *After deleting the* $i$*-th row and* $j$*-th column, the resulting submatrix* $\mathbf{Y}$ *is arbitrary permutation matrix of dimension* $N_{\mathrm{S}}-1$ *satisfying*

$$\begin{aligned}\sigma_{n-1}(\hat{\boldsymbol{\Sigma}}_{\mathrm{B}}\mathbf{Y}\hat{\boldsymbol{\Sigma}}_{\mathrm{F}}) &\ge \min_{i+j=n+1} \sigma_i(\mathbf{H}_{\mathrm{B}})\sigma_j(\mathbf{H}_{\mathrm{F}}) \text{ for } \mathbf{P},\\ \sigma_{n+1}(\hat{\boldsymbol{\Sigma}}_{\mathrm{B}}\mathbf{Y}\hat{\boldsymbol{\Sigma}}_{\mathrm{F}}) &\le \max_{i+j=n+N_{\mathrm{S}}} \sigma_i(\mathbf{H}_{\mathrm{B}})\sigma_j(\mathbf{H}_{\mathrm{F}}) \text{ for } \mathbf{Q},\end{aligned}$$

  *where* $\hat{\boldsymbol{\Sigma}}_{\mathrm{B}}$ *and* $\hat{\boldsymbol{\Sigma}}_{\mathrm{F}}$ *are diagonal singular value matrices of* $\mathbf{H}_{\mathrm{B}}$ *and* $\mathbf{H}_{\mathrm{F}}$ *with both* $i$*-th row and* $j$*-th column deleted, respectively.*

Corollary 3.3 and Proposition 2 both reveal the shaping limits of the $n$-th largest channel singular value, which may be used to simplify the MIMO precoder design with limited number $n$ of RF chains. They are derived under different assumptions are not special cases of each other. Importantly, Corollary 3.3 establishes upper and lower bounds for *each* channel singular value (c.f. first and last few in Proposition 2), applies to fully-connected BD-RIS of arbitrary size, and provides a general solution structure.

**Corollary 3.4** (Channel power gain)**.** *If the direct channel is negligible, then the channel power gain is bounded from above (resp. below) by the inner product of squared singular values of* $\mathbf{H}_{\mathrm{B}}$ *and* $\mathbf{H}_{\mathrm{F}}$ *when they are sorted similarly (resp. oppositely), that is,*

$$\sum_{n=1}^{N} \sigma_n^2(\mathbf{H}_{\mathrm{B}})\sigma_{N_{\mathrm{S}}-n+1}^2(\mathbf{H}_{\mathrm{F}}) \le \|\mathbf{H}\|_{\mathrm{F}}^2 \le \sum_{n=1}^{N} \sigma_n^2(\mathbf{H}_{\mathrm{B}})\sigma_n^2(\mathbf{H}_{\mathrm{F}}),$$

*whose upper and lower bounds are attained respectively at*

$$\begin{aligned}\boldsymbol{\Theta}_{\text{P-max}}^{\text{MIMO-ND}} &= \mathbf{V}_{\mathrm{B}}\mathbf{U}_{\mathrm{F}}^{\mathsf{H}},\\ \boldsymbol{\Theta}_{\text{P-min}}^{\text{MIMO-ND}} &= \mathbf{V}_{\mathrm{B}}\mathbf{J}\mathbf{U}_{\mathrm{F}}^{\mathsf{H}},\end{aligned}$$

*where* $\mathbf{J}$ *is the exchange (a.k.a. backward identity) matrix of dimension* $N_{\mathrm{S}}$.

We notice that (20a) and (20b) are special cases of (15a) and (15b) with $\mathbf{P}=\mathbf{I}$ and $\mathbf{Q}=\mathbf{J}$, which also attain the right and left halves of (18), respectively. The upper bound (20a) is also reminiscent of the optimal amplify-and-forward relay beamforming design [iv, (16), (17)] where the diagonal power allocation matrices boil down to $\mathbf{I}$ due to the passive nature of RIS.

**Corollary 3.5** (Channel capacity at general SNR)**.** *If the direct channel is negligible, then the BD-RIS aided MIMO channel capacity is*

$$C^{\text{MIMO-ND}}=\sum_{n=1}^{N}\log\left(1+\frac{s_n\sigma_n^2(\mathbf{H}_{\mathrm{B}})\sigma_n^2(\mathbf{H}_{\mathrm{F}})}{\eta}\right),$$

*where* $\eta$ *is the average noise power,* $s_n=\mu-\frac{\eta}{\sigma_n^2(\mathbf{H}_{\mathrm{B}})\sigma_n^2(\mathbf{H}_{\mathrm{F}})}$ *is the power allocated to the n-th mode obtainable by the water-filling algorithm [5]. The capacity-achieving BD-RIS scattering matrix is*

$$\boldsymbol{\Theta}_{\text{R-max}}^{\text{MIMO-ND}}=\mathbf{V}_{\mathrm{B}}\mathbf{U}_{\mathrm{F}}^{\mathsf{H}}.$$

Corollary 3.5 also suggests that the power gain- and rate-optimal scattering matrices (20a) and (23) coincide with each other when the direct channel is negligible and the BD-RIS is fully-connected. When either condition is not satisfied, active and passive beamforming are coupled and the rate-optimal solution involves alternating optimization. However, the power gain-optimal RIS still provides for a low-complexity decoupled solution. The details will be discussed in Section IV.

**Corollary 3.6** (Channel capacity at extreme SNR)**.** *If the direct channel is negligible, then the channel capacity when the SNR* $\rho$ *is very low and high are approximately bounded from above by*

$$C_{\rho_\downarrow}\lessapprox\sigma_1^2(\mathbf{H}_{\mathrm{B}})\sigma_1^2(\mathbf{H}_{\mathrm{F}}),$$
$$C_{\rho_\uparrow}\lessapprox N\log\frac{\rho}{N}+2\log\prod_{n=1}^{N}\sigma_n(\mathbf{H}_{\mathrm{B}})\sigma_n(\mathbf{H}_{\mathrm{F}}).$$

**1.6** *The optimization problems (39) and (36) lacks of novelty. In fact, they can still be solved by the methods proposed in existing literature, e.g., [i, 28] through appropriate adjustment.*

**Response** We agree with the reviewer that problem (36) may be solved by the method proposed in [i] with appropriate adjustment. We believe our method is more efficient as evident from Table I. However, although problem (39) has been studied in symmetric BD-RIS-aided Multiple-Input Single-Output (MISO) [28] where only one mode is available, generalizing those to MIMO is non-trivial due to trade-off between modes. We have also added a paragraph to clarify this point.

Problem (39) has been studied in Single-Input Single-Output (SISO) [25] and MISO equivalents [26, 28, 35, 39] where only one mode is available. Generalizing those to MIMO is non-trivial due to trade-off between modes.

**1.7** *Convergence proof in Appendix J is questionable. First, the manuscript just assumes that solution iterates* $\tilde{\boldsymbol{\Theta}}$ *converge. This may not be true (solution iterate could oscillate actually) and is hard to prove. Second, stationary point for constrained problem is more complicated than for the non-constrained case (e.g. gradient equals zero). Please refer to [v].*

**Response** We appreciate the reviewer for pointing out the issue. Indeed, the sequence of iterates may oscillate and the convergence proof in the previous version was incorrect. We have revised the wording in Proposition 5 and clarified the condition when a stationary point can be reached. The proof in Appendix J has been updated accordingly.

**Proposition 5.** *Starting from any feasible* $\boldsymbol{\Theta}^{(0)}$*, the orthogonal projection of*

$$\mathbf{M}_g^{(r)} = \mathbf{H}_{\mathrm{B},g}^{\mathsf{H}} \left( \mathbf{H}_{\mathrm{D}} + \mathbf{H}_{\mathrm{B}} \mathrm{diag}\big(\boldsymbol{\Theta}_{[1:g-1]}^{(r+1)}, \boldsymbol{\Theta}_{[g:G]}^{(r)}\big) \mathbf{H}_{\mathrm{F}} \right) \mathbf{H}_{\mathrm{F},g}^{\mathsf{H}}$$

*onto the Stiefel manifold, given in the closed-form [56]*

$$\boldsymbol{\Theta}_g^{(r+1)} = \underset{\mathbf{X}_g \in \mathbb{U}^{L \times L}}{\operatorname{argmin}} \|\mathbf{M}_g - \mathbf{X}_g\|_{\mathrm{F}} = \mathbf{U}_g^{(r)} \mathbf{V}_g^{(r)\mathsf{H}},$$

*monotonically increases the objective function (39a), where* $\mathbf{U}_g^{(r)}$ *and* $\mathbf{V}_g^{(r)}$ *are any left and right singular matrices of* $\mathbf{M}_g^{(r)}$*. When (40) converges, (41) leads to a convergence of the objective function (39a) towards a stationary point.*

**Remark 2.** We emphasize that the singular matrices in the Singular Value Decomposition (SVD) are not uniquely defined. When a singular value has multiplicity $k$, the corresponding singular vectors can be any orthonormal basis of the $k$-dimensional subspace. Even if all singular values are distinct, the singular vectors of each can be scaled by a phase factor of choice. Consequently, all SVD-based RIS solutions in this paper are inherently non-unique.

**Remark 4.** While a rigorous proof remains intricate due to the non-uniqueness of SVD, there is strong empirical evidence from simulation result that (40) converges and (41) provides an optimal solution for vastly tested scenarios.

## Reviewer 2

This paper studies the potential of a group-connected BD-RIS to manipulate the MIMO channel in terms of singular values, power gain, and achievable rate. The analysis and optimization are based on the assumption of asymmetric and lossless RIS circuit network without mutual coupling. A geodesic design framework is proposed and tested on Pareto frontier shaping and joint beamforming problems. Some analytical bounds on channel singular values and power gain are also provided. Overall, it is a solid work with interesting results. I have some further comments for the authors' reference.

**2.1** *How practical is it to consider asymmetric reconfigurable BD-RIS? How much gain is expected over symmetric ones and at what cost?*

**Response** Asymmetric RIS may be built over asymmetric passive components (e.g., ring hybrids and branch-line hybrids). A 4-port ring hybrid is illustrated in the figure below [30].

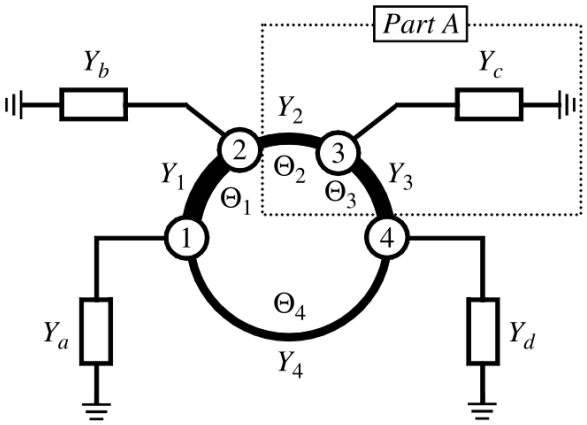


Fig. A 4-port asymmetric ring hybrid. Here the arc length between ports are $\Theta_1 = \Theta_2 = \Theta_3 = \lambda/4$ and $\Theta_4 = 3\lambda/4$ where $\lambda$ is the wavelength. The termination admittances $Y_a$ to $Y_d$ are arbitrary and the characteristic admittances of transmission-line sections are not necessarily the same, such that the scattering parameters can be asymmetric. Source: modified from [30].

On the other hand, symmetric RIS satisfying $\boldsymbol{\Theta} = \boldsymbol{\Theta}^{\mathsf{T}}$ are often considered in the literature as they can be implemented with simpler circuit components (e.g., capacitors and inductors). We have added Section V-D1 to investigate the impact of RIS symmetry on the system performance.

Symmetric RIS satisfying $\boldsymbol{\Theta} = \boldsymbol{\Theta}^{\mathsf{T}}$ are often considered in the literature due to hardware constraints. This study aim to investigate the impact of RIS symmetry on the system performance.

**Remark 5.** All proposed asymmetric BD-RIS designs can be modified for symmetry. In particular,

(i) *SVD-based (e.g., (15), (20), (23), (41), (44)):* Those closed-form asymmetric solutions are constructed from the product of singular matrices. If symmetry is required, one can replace the $\mathbf{U}, \mathbf{V}$ from the SVD of $\mathbf{A} = \mathbf{U}\boldsymbol{\Sigma}\mathbf{V}^{\mathsf{H}}$ by the factor $\mathbf{Q}$ from the Autonne-Takagi factorization of $\frac{\mathbf{A}+\mathbf{A}^{\mathsf{T}}}{2} = \mathbf{Q}\boldsymbol{\Sigma}\mathbf{Q}^{\mathsf{T}}$ [60] to construct the corresponding $\boldsymbol{\Theta}$;

(ii) *RCG-based (e.g., (26), (37)):* The symmetry constraint is added to the corresponding optimization problems, and one can project the solution to the nearest symmetric point $\boldsymbol{\Theta} \leftarrow \frac{\boldsymbol{\Theta}+\boldsymbol{\Theta}^{\mathsf{T}}}{2}$ after each iteration.

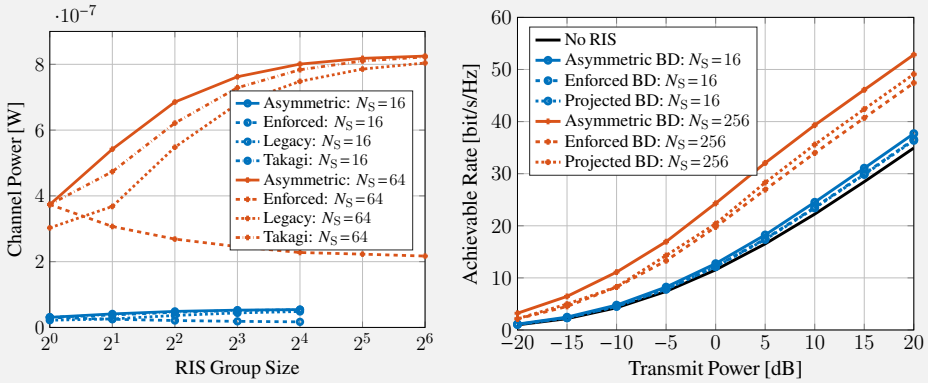


(a) Power: $2\times N_S\times 2$ (b) Rate: $4\times N_S\times 4$

Fig. Impact of RIS symmetry on the power gain and achievable rate of MIMO point-to-point channel.

Figs. 7a and 7b compare the power gain and achievable rate of MIMO point-to-point channel under asymmetric and various symmetric RIS configurations. Here, 'Asymmetric' refers to the benchmark solution by (41) or (37), 'Enforced' refers to enforcing symmetry on 'Asymmetric', 'Legacy' refers to a straightforward extension of the SISO SNR-optimal solution [28, (6)], 'Takagi' refers to the

modification (i), and 'Projection' refers to the modification (ii). We observe that the performance gaps between the asymmetric and symmetric RIS configurations are insignificant and tends to widen with the number of scattering elements. The two proposed modifications also outperform other candidates in both problems.

**2.2** *The geodesic RCG method seems promising especially at large group size L. Is it possible to extend the design framework to advanced BD-RIS architectures (e.g., multi-sector mode)?*

**Response** Unfortunately, the geodesic RCG method relies on the block unitary property of the BD-RIS scattering matrix and is not directly applicable to multi-sector mode BD-RIS where the constraint is relaxed to $\sum_{s=1}^{S} \mathbf{\Theta}_{g,s}^{\mathsf{H}} \mathbf{\Theta}_{g,s} = \mathbf{I}$, $\forall g \in [G]$ with $S > 1$ sectors.

**2.3** *For fully-connected BD-RIS, the authors mentioned in the result section that power gain-optimal scattering matrix is also rate-optimal. Can you provide a proof on this point?*

**Response** This is truly an interesting observation. When the direct channel is negligible and BD-RIS is fully-connected, the power gain-optimal and rate-optimal scattering matrices derived in closed form (20a) and (23) indeed coincide with each other. When the direct channel is significant, the observation still holds, yet we do not have a formal proof due to the non-trivial solution structures. The following context has been added to the manuscript to support this claim.

Corollary 3.5 also suggests that the power gain- and rate-optimal scattering matrices (20a) and (23) coincide with each other when the direct channel is negligible and the BD-RIS is fully-connected. When either condition is not satisfied, active and passive beamforming are coupled and the rate-optimal solution involves alternating optimization. However, the power gain-optimal RIS still provides for a low-complexity decoupled solution.

We also see that for fully-connected BD-RIS, the power gain-optimal and rate-optimal points coincide with each other, as have been proved in (20a) and (23). This observation still holds in Figs. 2(b) – 2(d) where the direct channel is significant, yet a formal proof is unavailable due to the non-trivial solution structures.

**2.4** *The authors refer to [32] for estimating forward and backward channels individually. However, it can be challenging to implement those in real time without RF chains at the RIS. The impact of imperfect Channel State Information (CSI) on the achievable rates may also be studied.*

**Response** We agree with the reviewer that the estimation of individual forward and backward channels may be challenging in practice. Section V-D2 has been added to investigate the impact of imperfect CSI on the proposed beamforming designs.

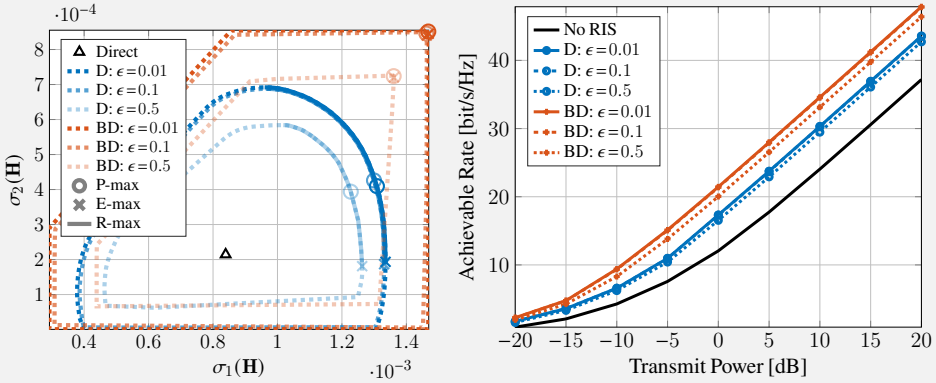


(c) Pareto: 2×64×2 (d) Rate: 4×128×4

Figure 3: Impact of RIS channel estimation error on the MIMO singular value region and achievable rate. A higher transparency of the Pareto frontier indicates a larger channel estimation error. 'D' means D-RIS and 'BD' refers to fully-connected BD-RIS.

Figs. 8(a) and 8(b) investigates how RIS channel estimation errors affect the system performance in terms of singular value region and achievable rate. We assume the direct channel can be perfectly acquired and the estimated backward and forward channels are modeled by

$$\hat{\mathbf{H}}_{\mathrm{B/F}} = \mathbf{H}_{\mathrm{B/F}} + \tilde{\mathbf{H}}_{\mathrm{B/F}},$$

where the error follows $\mathrm{vec}(\tilde{\mathbf{H}}_{\mathrm{B/F}}) \sim \mathcal{N}_{\mathbb{C}}(\mathbf{0}, \epsilon \Lambda_{\mathrm{B}} \Lambda_{\mathrm{F}} \mathbf{I})$. The results are evaluated over the ground truth channels. It is observed that the proposed channel shaping and joint beamforming solutions are reasonably robust to channel estimation errors. An interesting observation is that a BD-RIS designed over extremely poorly estimated channels ($\epsilon = 0.5$) may still outpeform a D-RIS designed over almost perfectly estimated channels ($\epsilon = 0.01$). We hope those results can motivate further research on the robust shaping design and provide insights for practical BD-RIS deployment.

**2.5** *Some sentences are confusing to me and the presentation can be improved. For example, "a group-wise geodesic RCG method that operates directly on the Stiefel manifold". Please elaborate more on this.*

**Response** Thank you for the feedback. The manuscript has been carefully restructured and proofread for improved clarity and readability.

## Reviewer 3

This paper analyzes the channel shaping of a Point-to-Point (P2P) MIMO system, assisted by passive diagonal and/or non-diagonal RISs to enhance power and rate gains. Overall, the topic is timely and interesting. Using Alternating Optimization (AO), a local optimal solution of the rate maximization for the BD-RIS-assisted MIMO P2P system is obtained. It is shown that BD-RIS improve the achievable rate. To the best of my knowledge, the analysis is solid. However, there are some suggestions for improving the paper further.

**3.1** *The results for the P2P system are insightful. However, a P2P system is not typically considered a practical system. It is challenging to extend the results to a system with interfering signals, where the goal is not only to enhance the channel gain of the desired links but also simultaneously to reduce the channel gain of the interfering links. It is more interesting to investigate the rate region of K-user Interference Channels (ICs). It is expected that the authors provide an analysis of the (max-min and sum) rate maximization of multi-user MIMO systems, assisted by BD-RISs.*

**Response** We appreciate the reviewer's positive feedback and insightful suggestion. Interference management by RIS in multi-user MIMO systems is indeed an interesting topic, but the page limit is a serious

concern and we have to prioritize the point-to-point content. The study on BD-RIS-aided interference channel deserves another submission and we are happy to share some initial results with you.

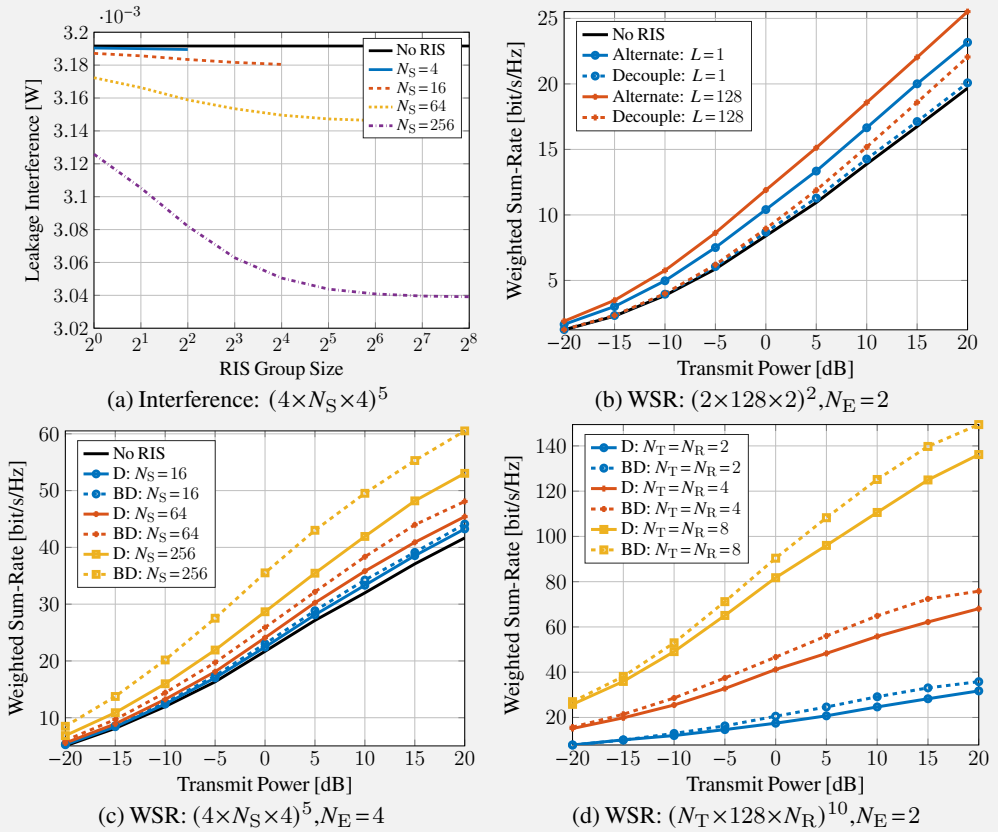


(a) Interference: $(4\times N_S\times 4)^5$

(b) WSR: $(2\times 128\times 2)^2, N_E=2$

(c) WSR: $(4\times N_S\times 4)^5, N_E=4$

(d) WSR: $(N_T\times 128\times N_R)^{10}, N_E=2$

Figure 4: Average leakage interference and weighted sum-rate versus RIS and MIMO interference channel configurations. 'Alternate' refers to the alternating optimization and 'Decouple' refers to the low-complexity design. 'D' means D-RIS and 'BD' refers to fully-connected BD-RIS.

Fig. 4a illustrates how BD-RIS helps to reduce the leakage interference. In this case, a fully-connected $2^n$-element BD-RIS is almost as good as a $2^{n+2}$-element D-RIS in terms of leakage interference. The result also implies that BD-RIS can achieve a higher DoF than diagonal RIS in MIMO interference channel, which generalizes Proposition 1 and emphasizes the potential of BD-RIS in interference alignment.

Fig. 4b compares the average Weighted Sum-Rate (WSR) achieved by the optimal and low-complexity beamforming designs, respectively. Unlike the point-to-point case, the latter is not as effective as the former. The reason is that, for $K$ transmissions of different path loss, interference alignment using only a shared passive beamformer is very challenging especially, when the direct channels are dominant. On the other hand, using $K$ precoders in the joint beamforming design can reasonably orthogonalize the channels and the RIS can simply enhance the signal power. A narrower performance gap is expected when $N_S$ increases or RIS coverage area shrinks.

Figs. 4c and 4d show the average WSR versus the number of scattering elements and transceiving antennas. Again, we observe that the rate gain of BD-RIS over D-RIS increases with $N_S$, $N_T$, and $N_R$. The reasons have been discussed in the point-to-point case.

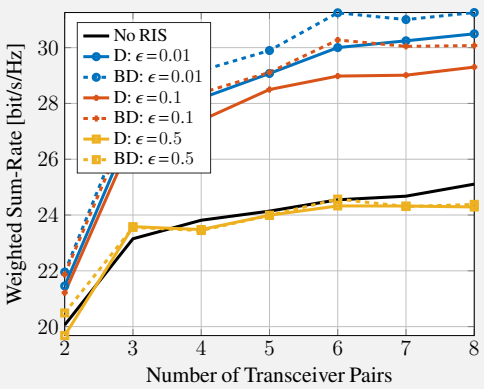


Figure 5: Impact of channel estimation error and transceiver pairs on the weighted sum-rate of $(2\times64\times2)^K$ MIMO interference channel with $P=20\text{dB}$ and $N_{\text{E}}=2$.

Fig. 5 shows the average WSR versus the backward/forward channel estimation error and the number of transceiver pairs. Specifically, the active and passive beamformers are designed over the estimated backward and forward channels

$$\hat{\mathbf{H}}_{\text{B/F}}^{(k)}=\mathbf{H}_{\text{B/F}}^{(k)}+\tilde{\mathbf{H}}_{\text{B/F}}^{(k)},\quad \forall k,$$

where the error follows $\text{vec}(\tilde{\mathbf{H}}_{\text{B/F}}^{(k)})\sim\mathcal{N}_{\mathbb{C}}(\mathbf{0},\epsilon\Lambda_{\text{B}}\Lambda_{\text{F}}\mathbf{I})$. The WSR is evaluated using the true channels. We observe that the proposed joint beamforming design is reasonably robust to channel estimation error and thus viable for practical implementation. On the other hand, introducing a RIS to interference channel systems is helpful to mitigate the rate saturation effect as $K$ increases. In the saturated regime ($K\geq4$), BD-RIS provides a much larger WSR than D-RIS thanks to its superior shaping capability in aligning the interference subspaces. These results provide valuable insights for practical RIS design in dense connection scenarios, where proper BD configurations can significantly enhance the network capacity.

**3.2** *BD-RISs provide a greater number of optimization variables but at the expense of increased computational and implementation complexities. While the computational complexities of the proposed solutions are discussed in the paper, a comparison with D-RIS is missing, which should be explicitly addressed in both the introduction and the main body. Additionally, the implementation complexities of BD-RISs, particularly in comparison to D-RIS, necessitate a more comprehensive analysis. For instance, as highlighted in [vi], the energy efficiency of a BD-RIS is significantly influenced by the static power consumption of its circuit elements. If the implementation cost of a BD-RIS is substantial, its performance advantages could be considerably reduced.*

**Response** We agree with the reviewer that the computational complexities of D-RIS and fully-connected BD-RIS deserve further attention. Apart from a summary in the introduction and an explicit analysis in the main body, we have also evaluated the average statistics of the AO design for both architectures on the rate maximization problem (35).

On the other hand, the implementation complexities of BD-RIS is indeed a critical issue. An initial study has been conducted in [36] where the authors demonstrated the superior energy efficiency of BD-RIS compared to both active RIS and relay systems. Our colleagues are currently working on a more comprehensive analysis and the results will be published in a separate paper.

The additional optimization cost of BD-RIS over D-RIS is affordable and the geodesic RCG method is efficient on large-scale problems;

That is, $O_{\text{D}}\left(N_{\text{S}}\right)$ for D-RIS and $O_{\text{BD}}\left(N_{\text{S}}^3\right)$ for fully-connected BD-RIS.

Table: Performance of D-RIS and Fully-Connected BD-RIS on (35)

| RIS type | $N_{\mathrm{S}}=16$ | | | $N_{\mathrm{S}}=256$ | | |
|---|---|---|---|---|---|---|
| | Objective | Iterations (outer) | Time [s] | Objective | Iterations (outer) | Time [s] |
| Diagonal | 25.33 | 2.06 | $2.620\times10^{-2}$ | 32.22 | 2.92 | 1.277 |
| Fully-connected BD | 26.10 | 3.84 | $2.719\times10^{-2}$ | 36.58 | 3.03 | 0.806 |

Table II compares the performance of D-RIS and fully-connected BD-RIS on rate maximization problem (35) using the AO design in Section IV-A, where $N_{\mathrm{T}}=N_{\mathrm{R}}=4$ and $P=20\mathrm{dB}$. The statistics are averaged over 100 independent runs. The fact that fully-connected BD-RIS provides a higher achievable rate using slightly more outer iterations $I_{\mathrm{AO}}$ than D-RIS is consistent with our analysis. Interestingly, *the former still ends up with shorter elapsed time,* which seems to contradict the complexity analysis that $O_{\mathrm{BD}}\left(N_{\mathrm{S}}^3\right)$ for fully-connected BD-RIS and $O_{\mathrm{D}}\left(N_{\mathrm{S}}\right)$ for D-RIS. One possible reason is that BD-RIS only involves 1 backtracking line search per iteration while D-RIS requires $N_{\mathrm{S}}$ times. Another reason is that the group-wise update of D-RIS leads to slower convergence of inner iterations. These results suggest that optimizing BD-RIS may be less computational intensive than expected.

**3.3** *The authors considered a passive RIS architecture. However, another passive configuration, termed Globally Passive (GP), is discussed in [vii, viii]. Employing AO, the resulting optimization problem to update* $\boldsymbol{\Theta}$ *is convex. Comparing the proposed solutions with a globally passive BD-RIS would provide valuable insights into the performance gains obtained by relaxing the (locally) passive assumption. Hence, it is highly recommended to add the GP (both BD and diagonal) architecture as a benchmark in the numerical results.*

**Response** We appreciate the reviewer's suggestion and agree that the GP architecture may serve as a canonical benchmark. However, the current manuscript already exceeds the page limit and we decided not to overwhelm the readers with too many fancy RIS configurations. An in-depth comparison between GP and BD architectures holds significant value to the RIS community and deserves a separate study in the future.

## References


[i] H. Li, S. Shen, and B. Clerckx, "Beyond diagonal reconfigurable intelligent surfaces: From transmitting and reflecting modes to single-, group-, and fully-connected architectures," *IEEE Transactions on Wireless Communications*, vol. 22, pp. 2311–2324, Apr 2023.

[ii] J.-F. Cai, E. J. Candès, and Z. Shen, "A singular value thresholding algorithm for matrix completion," *SIAM Journal on Optimization*, vol. 20, no. 4, pp. 1956–1982, 2010.

[iii] Y. Rong and F. Gao, "Optimal beamforming for non-regenerative MIMO relays with direct link," *IEEE Communications Letters*, vol. 13, no. 12, pp. 926–928, Dec 2009.

[iv] Y. Rong and Y. Hua, "Optimality of diagonalization of multi-hop MIMO relays," *IEEE Transactions on Wireless Communications*, vol. 8, no. 12, pp. 6068–6077, Dec 2009.

[v] J.-S. Pang, M. Razaviyayn, and A. Alvarado, "Computing B-stationary points of nonsmooth DC programs," *Mathematics of Operations Research*, vol. 42, no. 1, pp. 95–118, Jan 2017.

[vi] M. Soleymani, I. Santamaria, E. Jorswieck, M. Di Renzo, and J. Gutiérrez, "Energy efficiency comparison of RIS architectures in MISO broadcast channels," in *2024 IEEE 25th International Workshop on Signal Processing Advances in Wireless Communications (SPAWC)*. IEEE, Sep 2024, pp. 701–705.

[vii] R. K. Fotock, A. Zappone, and M. D. Renzo, "Energy efficiency optimization in RIS-aided wireless networks: Active versus nearly-passive RIS with global reflection constraints," *IEEE Transactions on Communications*, vol. 72, no. 1, pp. 257–272, 2024.

[viii] M. Soleymani, A. Zappone, E. Jorswieck, M. D. Renzo, and I. Santamaria, "Rate region of RIS-aided URLLC broadcast channels: Diagonal versus beyond diagonal globally passive RIS," *IEEE Wireless Communications Letters*, pp. 1–1, 2024.